Journal of Solid Mechanics Vol. 14, No. 2 (2022) pp. 147-170
DOI: 10.22034/jsm.2021.1907364.1635

Elasticity Exact Solution for an FGM Cylindrical Shaft with Piezoelectric Layers Under the Saint-Venant Torsion by Using Prandtl's Formulation

M.R. Eslami [1], M. Jabbari [2], A. Eskandarzadeh Sabet [2,*]

[1]*Mechanical Engineering Department, Amirkabir University of Technology, Tehran, Iran*
[2]*Mechanical Engineering Department, Postgraduate School, Islamic Azad University, South Tehran Branch, Iran*

Received 9 February 2022; accepted 29 March 2022

ABSTRACT
Functionally graded materials (FGMs) belong to a noble family of composite material possess material properties varying gradually in a desired direction or orientation. In a past decade, functionally graded materials were remained in an interest of material investigators due to its prominent features, and have extensively used in almost every discipline of engineering which in turn significantly increases the number of research publication of FGM. In this paper the exact elasticity solution for an FGM circular shaft with piezo layers is analysed. piezoelectric layers are homogeneous and the modulus of elasticity for FGM varies continuously with the form of an exponential function. The shear modulus of the non-homogeneous FGM shaft is a given function of the Prandtl's stress function of considered circular shaft when its material is homogeneous. state equations are derived. The Prandtl's stress function and electric displacement potential function satisfy all conditions. The shearing stresses, torsional rigidity, torsional function for FGM layer and shearing stresses, electric displacements, torsional rigidity, electrical torsional rigidity, torsional and electrical potential functions for piezoelectric layers are obtained. Exact analytical solution for hollow circular cross-section presented. At the end some graphs and conclusions are given.

Keywords: FGM (functionally graded material); Piezoelectric; Elasticity; Torsion; Cylindrical shaft; Exact solution.

1 INTRODUCTION

THE FGM(functionally graded material) was first considered in Japan in 1984. Appropriate macroscopically inhomogeneous phase concentrations, and particle morphologies and orientation distributions have recently been applied in a variety of fields, including aircraft, aerospace, and automobile technologies, heat exchanger tubes, thermoelectric generators and heat-engine components [1]. The properties of FGM vary smoothly and continuously

*Corresponding author.
E-mail address: st_a_eskandarzadeh@azad.ac.ir (A. Eskandarzadeh Sabet)

from one surface to the other [2]. In many cases, properties change between metal and ceramic phases. The ceramic in a FGM provides insulation against heat and protects the metal from corrosion and oxidation while the FGM is strengthened by the metallic composition. As a result, these materials are able to withstand high temperature gradients without structural failures [3]. Piezoelectricity was first discovered by Jacques and Pierre Curie in 1880. Piezoelectric materials have various applications because of their unique behavior. Piezoelectric effect is an interaction between electrical and mechanical state of some materials [4]. As a result, these materials can be used in sensors and actuators and wherever there is a need for electromechanical interactions, These materials should have crystals with no inversion symmetry in order to exhibit piezoelectric properties [4].Torsional problems have a great importance in structural analysis and design of mechanical parts [4].Torsion is an important factor in the design of some load carrying elements such as shafts, curved beams, edge shafts in buildings, and eccentrically loaded bridge girders [5]. In recent years, the composition of several different materials has been often used in structural components in order to optimize responses of the structures subjected to thermal and mechanical loads. Saint-Venant's torsion of a homogeneous, isotropic or anisotropic elastic circular bar is a classical problem of elasticity which was solved using the semi-inverse method by assuming a state of pure shear in the body such that it gives rise to a resultant torque over the end section [6]. Also, Saint-Venant's torsion of a non-homogeneous circular bar was solved, in this method the solutions of homogeneous torsion problems are employed to find solutions corresponding non-homogeneous problems. Saint-Venant's torsion of a homogeneous, monoclinic piezoelectric shaft is formulated in terms of Prandtl's function and electric displacement potential function. In all cases of Saint–Venant's torsion mention above the states of strains and stresses are independent of the axial coordinate. Following Saint–Venant it is assumed that the character of elastic and electric fields depends only in a secondary way of the exact distribution of the tractions on the ends of cylinder so that the end torques are introduced in an integral manner in the case of torsional problem [7]. Saint-venant's torsion of a homogeneous isotropic, elastic cylindrical body was solved by Higgins [8], Timoshenko and Goodier [9], Sokolnikoff [10]. A novel class of graded cylinders is proposed by Chen [11] as neutral inclusions inside host shafts of arbitrary cross section under Saint-Venant's torsion. Baron [12] studied torsion of hollow tubes by multiplying the connected cross sections, He used an iterative method to satisfy the equilibrium and compatibility equations. A computational method for calculating torsional stiffness of multi-material bars with arbitrary shape was studied by Li et al. [13], In this work, they considered additional compatibility and equilibrium equations in common boundaries of different materials in their formulation and got good results. Mijak [14] considered a new method to design an optimum shape in beams with torsional loading, In his work, cost function was torsional rigidity of the domain and constraint was the constant area of the cross-section while shape parameters were co-ordinates of the finite element nodes along the variable boundary, The problem was solved directly by optimizing the cost function with respect to the shape parameters. He solved this problem using finite elements (FE) method. Kubo and Sezawa [15] presented a theory for calculating the torsional buckling of tubes and also reported on experimental results for rubber models. However, this theory did not show an agreement with experimental results. Lundquist [16] performed extensive experiments on the strength of aluminum shafts under torsion reported in 1932. Recently, Doostfatemeh et al. [17] obtained a closed-form approximate formulation for torsional analysis of hollow tubes with straight and circular edges. In this work, the problem was formulated in terms of Prandtl's stress function. Also, accuracy of the formulas was verified by accurate finite element method solutions. Muskhelishvilli [18] presented the governing equation and boundary condition of the torsion of composite bars and its solution in Fourier series for composite section with two sub-rectangles. This solution was extended later for multiple rectangular composite section by Booker and Kitipornchai [19]. Kuo and Conway [20–23] analyzed the torsion of the composite sections of various shapes. Packham and Shail [24] extended their work on two-phase fluid to the torsion of composite shafts. Ripton [25] investigated the torsional rigidity of composite section reinforced by fibers. Herrmann [26] utilized the finite element method to calculate the warping function of the torsion of irregular sectional shapes. Torsion of elastic circular bars of radially inhomogeneous, cylindrically orthotropic materials is studied with emphasis on the end effects by Tarn and Chang [27]and compared their method with Saint-Venant's torsion. anisotropic or non-homogeneous materials has been considered by Lekhnitskii [28,29],Rooney and Ferrari [1], Bisegna [30,31]and Horgan [32]. The formulation of the theory of uniform torsion for piezoelectric shafts has been analysed by Bisegna [30,31], Rovenski et al.[33,34],Yang [35], a relaxed version of this problem including the torsion is also formulated and solved by Bisegna [30,31].The papers by Bisegna [30,31] use the Prandt'ls stress function and electric displacement potential function formulation for simply-connected cross-sections which is based on Clebsch-type hypothesis. Tawaka et al. [36] studied torsional vibration control with piezoelectric actuation. Zehetner [37] studied compensation of torsion in rods by piezoelectric actuation. Maleki et al. [38] presented exact three-dimensional analysis for torsion of piezoelectric rods. Rovenski et al.[33,34]give the torsional and electric potential function formulation of the saint-venant's torsional problem for monoclinic piezoelectric shafts.In the papers by Rovenski et al.[33,34] a coupled Neumann problem is derived for the torsional and electric potential functions, where exact and numerical solutions for elliptical and rectangular cross-sections are presented. Torsion of circular cylinders made of ceramics with tangential poling is studied by Yang [35]. In the paper Ecsedi et al. [7] the Saint–Venant's torsional problem is formulated in the framework of the linear theory of piezoelectricity for homogeneous, monoclinic piezoelectric cylinders with arbitrary cross-sectional geometry, the Prandtl's stress function and electric displacement potential function formulation is developed for multiply-connected cross-sections [7].

In this paper, piezoelastic solution for an FGM cylindrical shaft with piezo layers under the Saint-Venant's torsion is presented, piezoelectric layers for solved example are homogeneous(Although obtained relations also satisfies the non-homogeneous state) and length is finite.Influence of layers together applied, all results about the Saint-Venant's torsion which is solved,verified.Finally,the obtained state equations are solved, and the stresses, electric displacements, torsional functions,electric potential functions are presented. The Sadd [39] results about the Saint-Venant's torsion are recovered in sections 2.1 and 2.1.1 for FGM layer, here Prandtl's stress function is introduced, expressions for displacement single value condition, torsional function and torsional rigidity are also presented. The base of the study about the piezoelectric layers is section 2.2 that formulates the governing field equations and boundary conditions of the Saint–Venant's torsional problem for piezoelectric shafts by the use of results of Rovenski et al. [33]. In section 2.2.1, Prandtl's stress function and electric displacement potential function are introduced, here the expressions for torsional and electric potential functions in terms of Prandtl's stress function and electric displacement potential function are also presented with the equations of coupled Dirichlet boundary-value problem, torsional and electric potential functions are single valued. In section 2.2.2 torsional rigidity and electric torsional rigidity are presented. Formulas for Continuously Conditions which shows Influence layers on together are derived in section 3. the electric potential between surfaces FGM and piezo is zero. Section 4 contains one exact analytical example for hollow circular cross-section. Some Graphs and conclusions are given in sections 5 and 6 respectively.

2 STATE-SPACE FORMULATION

Consider a functionally graded cylindrical panel with non-homogeneous mechanical properties in exponential form that is bounded with piezoelectric layers (Fig. 1).

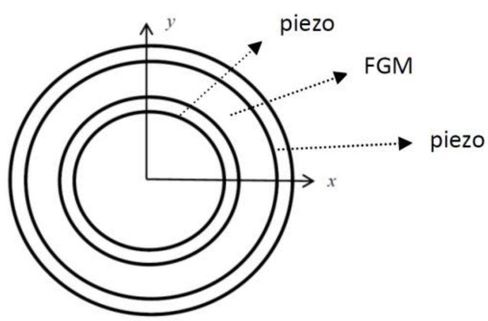

Fig.1
Piezo-FGM cross-section.

2.1 FGM layer [39]

Displacements can be determined as:

$$u = -r\beta sin\theta = -\beta y \tag{1}$$

$$v = r\beta cos\theta = \beta x \tag{2}$$

Using the assumption that the section rotation is a linear function of the axial coordinate, we can assume that the cylinder is fixed at $z = 0$ and take

$$\beta = \alpha z \tag{3}$$

where the parameter α is the angle of twist per unit length. Collecting these results together, the displacements for the torsion problem can thus be written as:

$$\begin{aligned} u &= -\alpha yz \\ v &= \alpha xz \\ \omega &= \omega(x, y) \end{aligned} \tag{4}$$

2.1.1 Stress-stress function formulation for isotropic non-homogeneous material [39]

$$\begin{aligned} e_x &= e_y = e_z = e_{xy} = 0 \\ e_{xz} &= \frac{1}{2}\left(\frac{\partial \omega}{\partial x} - \alpha y\right) \\ e_{yz} &= \frac{1}{2}\left(\frac{\partial \omega}{\partial y} + \alpha x\right) \end{aligned} \tag{5}$$

The corresponding stresses follow from Hooke's law:

$$\begin{aligned} \sigma_x &= \sigma_y = \sigma_z = \tau_{xy} = 0 \\ \tau_{xz} &= \mu\left(\frac{\partial \omega}{\partial x} - \alpha y\right) \\ \tau_{yz} &= \mu\left(\frac{\partial \omega}{\partial y} + \alpha x\right) \end{aligned} \tag{6}$$

For the state that body forces is zero, the equilibrium equations reduce to:

$$\frac{\partial \tau_{xz}}{\partial x} + \frac{\partial \tau_{yz}}{\partial y} = 0 \tag{7}$$

$$\tau_{xz} = \frac{\partial \phi}{\partial y} \qquad \tau_{yz} = -\frac{\partial \phi}{\partial x} \tag{8}$$

We can generate the compatibility relation among the two nonzero stress components by differentiating and combining relations $(6)_{2,3}$ to eliminate the displacement terms. Substituting relation (8) into that result gives the governing relation in terms of the stress function

$$\frac{\partial}{\partial x}\left(\frac{1}{\mu}\frac{\partial \phi}{\partial x}\right) + \frac{\partial}{\partial y}\left(\frac{1}{\mu}\frac{\partial \phi}{\partial y}\right) = -2\alpha \tag{9}$$

where the shear modulus μ must now be left inside the derivative operations because the material is inhomogeneous. The components of the unit normal vector can be expressed as:

$$n_x = \frac{dy}{ds} = \frac{dx}{dn} \quad , \quad n_y = -\frac{dx}{ds} = \frac{dy}{dn} \tag{10}$$

To complete the stress formulation must apply the boundary conditions on the problem. If the lateral surface of the cylinder s is to be free of traction, and thus

$$\begin{aligned} T_x^n &= \sigma_x n_x + \tau_{yx} n_y + \tau_{zx} n_z = 0 \\ T_y^n &= \tau_{xy} n_x + \sigma_y n_y + \tau_{zy} n_z = 0 \\ T_z^n &= \tau_{xz} n_x + \tau_{yz} n_y + \sigma_z n_z = 0 \end{aligned} \tag{11}$$

The first two relations are identically satisfied because $\sigma_x = \sigma_y = \tau_{xy} = n_z = 0$,and by using Eq. (8) in Eq.(11)$_3$, have

$$\begin{aligned} &\tau_{xz} n_x + \tau_{yz} n_y = 0 \\ &\frac{\partial \phi}{\partial x}\frac{dx}{ds} + \frac{\partial \phi}{\partial y}\frac{dy}{ds} = 0 \\ &\frac{d\phi}{ds} = 0 \end{aligned} \tag{12}$$

with regard to the stress function, the value of ϕ may be arbitrarily chosen only on one boundary, and commonly this value is taken as zero on the outer boundary, but in this paper it is much different and refer in the next part (since have 3 layers together). Next consider the boundary conditions on the ends of the cylinder, on this boundary, components of the unit normal become $n_x = n_y = 0, n_z = \pm 1$ so

$$\begin{aligned} T_x^n &= \pm \tau_{xz} \\ T_y^n &= \pm \tau_{yz} \\ T_z^n &= 0 \end{aligned} \tag{13}$$

Moment should be a pure torque *T* about the *z*-axis. This condition is specified by

$$T = \iint_R \left(x T_y^n - y T_x^n \right) dxdy = -\iint_R \left(x \frac{\partial \phi}{\partial x} + y \frac{\partial \phi}{\partial y} \right) dxdy \tag{14}$$

Using results from Green’s theorem

$$\iint_R x \frac{\partial \phi}{\partial x} dxdy = \iint_R \frac{\partial}{\partial x}(x\phi) dxdy - \iint_R \phi dxdy = \oint_s x\phi n_x ds - \iint_R \phi dxdy \tag{15}$$

$$\iint_R y \frac{\partial \phi}{\partial y} dxdy = \iint_R \frac{\partial}{\partial y}(y\phi) dxdy - \iint_R \phi dxdy = \oint_s y\phi n_y ds - \iint_R \phi dxdy \tag{16}$$

Because ϕ is not zero on *S*, the boundary integrals in (15) and (16) will not vanish and relations (15) and (16) is

$$T = 2\iint_R \phi dxdy + \sum_{k=1}^{N} 2\phi_k A_k \tag{17}$$

$$J = \frac{T}{\alpha} \tag{18}$$

N is number of holes that ϕ is not zero. For multiply connected sections, the constant values of the stress function on each of boundaries are determined by requiring that the displacement *w* be single-valued. Considering the multiply connected ,the displacement will be single-valued if

$$\oint_{s_1} dw\left(x,y\right)=0 \qquad \oint_{s_2} dw\left(x,y\right)=0 \qquad \oint_{s_k} dw\left(x,y\right)=0 \tag{19}$$

$$\oint_{s_1} dw\left(x,y\right)=\oint_{s_1}\left(\frac{\partial w}{\partial x}dx+\frac{\partial w}{\partial y}dy\right)=\frac{1}{\mu}\oint_{s_1}(\tau_{xz}dx+\tau_{yz}dy)-\alpha\oint_{s_1}\left(xdy-ydx\right) \tag{20}$$

Now $\tau_{xz}dx+\tau_{yz}dy=\tau ds$, where τ is the resultant shear stress. Using Green's theorem

$$\oint_{s_1}\left(xdy-ydx\right)=\iint_{A_1}\left(\frac{\partial x}{\partial x}+\frac{\partial y}{\partial y}\right)dxdy=2\iint_{A_1}dxdy=2A_1 \tag{21}$$

where A_1 is the area enclosed by S_1. Combining these results, the single-valued condition (19) implies that

$$\oint_{s_1}\frac{\tau ds}{\mu}=2\alpha A_1 \tag{22}$$

$$\oint_{s_2}\frac{\tau ds}{\mu}=2\alpha A_2 \tag{23}$$

The value of ϕ on the inner boundary *S* must therefore be chosen so that (22) and (23) are satisfied.

$$\oint_{s_k}\frac{\tau ds}{\mu}=2\alpha A_k \tag{24}$$

where *k* is related to each surface that ϕ is not zero(inner and outer boundary of shaft to state that is bounded by two layers).

2.2 Piezoelectric layers

In this part only one piezoelectric layer investigated, torsional problem provide form displacement and potential hypothesis [33,34,7]

$$u=-\alpha yz \qquad v=\alpha xz \qquad w=\alpha\omega\left(x,y\right) \quad \varphi=\alpha\psi\left(x,y\right) \tag{25}$$

where Eq.(25) are the displacements in *x, y* and *z* directions. $\omega\left(x,y\right)$ is the torsional function and ψ is electric potential function. The strain-displacement and electric field-electric potential relationships give [10,11,12,13,17]

$$\varepsilon_x=\varepsilon_y=\varepsilon_z=\varepsilon_{xy}=0 \qquad \varepsilon_{xz}=\alpha\left(\frac{\partial\omega}{\partial x}-y\right) \qquad \varepsilon_{yz}=\alpha\left(\frac{\partial\omega}{\partial y}+x\right) \tag{26}$$

$$E_x=-\alpha\frac{\partial\psi}{\partial x} \qquad E_y=-\alpha\frac{\partial\psi}{\partial y} \qquad E_z=0 \tag{27}$$

E_x, E_y, E_z are the components of electric field in Cartesian coordinate and because of φ is a function of $\left(x,y\right)$, $E_z=0$ and the partial differentiation is assumed in the radial direction(E_x, E_y)That, $\varepsilon_x, \varepsilon_y, \varepsilon_z$ are the longitudinal strains, $\varepsilon_{xy}, \varepsilon_{xz}, \varepsilon_{yz}$ are the shearing strains, E_x, E_y, E_z are the components of electric field. mechanical equilibrium and gauss equation in two dimension are [33,34,7]

$$\frac{\partial \tau_{xz}}{\partial x}+\frac{\partial \tau_{yz}}{\partial y}=0 \qquad \frac{\partial D_x}{\partial x}+\frac{\partial D_y}{\partial y}=0 \quad \text{in } R \tag{28}$$

τ_{xz}, τ_{yz} are the shearing stresses, D_x, D_y are the components of electric displacement. Here we have [10,11].

$$\sigma_x=\sigma_y=\sigma_z=\tau_{xy}=0 \quad \text{and } D_z=0 \tag{29}$$

where, $\sigma_x, \sigma_y, \sigma_z$, are the normal stresses, and in Eq.(28) we have no body forces and body. If the no layer is not on the piezo layer have [7]

$$\tau_{xz} n_x+\tau_{yz} n_y=0, \qquad D_x n_x+D_y n_y=0 \quad \text{on } S \tag{30}$$

Assuming that the considered shaft is made of monoclinic piezoelectric material have [12,13,17]

$$\varepsilon_{xz}=s_{55}\tau_{xz}+s_{45}\tau_{yz}+g_{15}D_x+g_{25}D_y \tag{31}$$

$$\varepsilon_{yz}=s_{45}\tau_{xz}+s_{44}\tau_{yz}+g_{14}D_x+g_{24}D_y \tag{32}$$

$$E_x=-\frac{\partial \psi}{\partial x}=-g_{15}\tau_{xz}-g_{14}\tau_{yz}+\eta_{11}D_x+\eta_{12}D_y \tag{33}$$

$$E_y=-\frac{\partial \psi}{\partial y}=-g_{25}\tau_{xz}-g_{24}\tau_{yz}+\eta_{12}D_x+\eta_{22}D_y \tag{34}$$

s_{55}, s_{45}, s_{44} are the flexibility coefficients, g_{15}, g_{25}, g_{24}, are the piezoelectric impermeability coefficients and $\eta_{11}, \eta_{12}, \eta_{22}$ are the dielectic impermeability coefficients.

2.2.1 Prandtl's stress function and electric displacement potential function formulation

Let $\phi=\phi(x, y)$ and $F=F(x, y)$ be such functions whose second order mixed partial derivatives are the same according to young's theorem, but they are otherwise arbitrary functions. The general solution of Eq. (28) by these functions is presented as [7,40]:

$$\begin{gathered}\frac{\partial \tau_{xz}}{\partial x}+\frac{\partial \tau_{yz}}{\partial y}=\alpha \frac{\partial^2 \phi}{\partial x \partial y}-\alpha \frac{\partial^2 \phi}{\partial x \partial y}=0 \qquad \frac{\partial D_x}{\partial x}+\frac{\partial D_y}{\partial y}=\alpha \frac{\partial^2 F}{\partial x \partial y}-\alpha \frac{\partial^2 F}{\partial x \partial y}=0 \\ \tau_{xz}=\alpha \frac{\partial \phi}{\partial y} \qquad \tau_{yz}=-\alpha \frac{\partial \phi}{\partial x} \quad D_x=\alpha \frac{\partial F}{\partial y} \qquad D_y=-\alpha \frac{\partial F}{\partial x}\end{gathered} \tag{35}$$

$\phi=\phi(x, y)$ is called the Prandtl's stress function and $F=F(x, y)$ is electric displacement potential function. From Eq. (28) we have [7]

$$\alpha \frac{\partial \phi}{\partial y}\frac{dy}{ds}+\alpha \frac{\partial \phi}{\partial x}\frac{dx}{ds}=0 \qquad \alpha \frac{\partial F}{\partial y}\frac{dy}{ds}+\alpha \frac{\partial F}{\partial x}\frac{dx}{ds}=0 \quad \text{on } S \tag{36}$$

$$\frac{d\phi}{ds}=0 \qquad \frac{dF}{ds}=0 \quad \text{on } S \tag{37}$$

It means that

$$\phi = \phi_i = constant \quad \text{on } S_i \left(i = 0 - p\right) \tag{38}$$

$$F = F_i = constant \quad \text{on } S_i \left(i = 0 - p\right) \tag{39}$$

with regard to the stress function and electric displacement potential function, the value of ϕ and F may be arbitrarily chosen only on one boundary, and commonly this values is taken as zero on the outer boundary, but in this paper it is much different and refer in the next part.

$$\phi = \phi_0 = 0 \quad \text{and} \quad F = F_0 = 0 \quad \text{on } S_0 \tag{40}$$

The combination of Eqs. (26) and (27) with Eqs. (31)-(34) and Eq.(35) gives

$$\begin{bmatrix} -\dfrac{\partial \omega}{\partial y} - x \\ \dfrac{\partial \omega}{\partial x} - y \end{bmatrix} = \begin{bmatrix} s_{44}\dfrac{\partial \phi}{\partial x} - s_{45}\dfrac{\partial \phi}{\partial y} \\ -s_{45}\dfrac{\partial \phi}{\partial x} + s_{55}\dfrac{\partial \phi}{\partial y} \end{bmatrix} + \begin{bmatrix} g_{24}\dfrac{\partial F}{\partial x} - g_{14}\dfrac{\partial F}{\partial y} \\ -g_{25}\dfrac{\partial F}{\partial x} + g_{15}\dfrac{\partial F}{\partial y} \end{bmatrix} \tag{41}$$

$$\begin{bmatrix} -\dfrac{\partial \psi}{\partial y} \\ \dfrac{\partial \psi}{\partial x} \end{bmatrix} = \begin{bmatrix} g_{24}\dfrac{\partial \phi}{\partial x} - g_{25}\dfrac{\partial \phi}{\partial y} \\ -g_{14}\dfrac{\partial \phi}{\partial x} + g_{15}\dfrac{\partial \phi}{\partial y} \end{bmatrix} - \begin{bmatrix} \eta_{22}\dfrac{\partial F}{\partial x} - \eta_{12}\dfrac{\partial F}{\partial y} \\ -\eta_{12}\dfrac{\partial F}{\partial x} + \eta_{11}\dfrac{\partial F}{\partial y} \end{bmatrix} \tag{42}$$

The torsional function $\omega = \omega\left(x, y\right)$ and the electric potential function $\psi = \psi\left(x, y\right)$ are single valued functions so we have

$$\oint_{s_1} d\,\omega\left(x, y\right) = 0 \qquad \oint_{s_1} d\psi\left(x, y\right) = 0 \tag{43}$$

The upper integrals can be written as:

$$\oint_{s_1} [(-s_{44}\frac{\partial \phi}{\partial x} + s_{45}\frac{\partial \phi}{\partial y} - g_{24}\frac{\partial F}{\partial x} + g_{14}\frac{\partial F}{\partial y}) \times \frac{dy}{ds} + \left(+s_{45}\frac{\partial \phi}{\partial x} - s_{55}\frac{\partial \phi}{\partial y} + g_{25}\frac{\partial F}{\partial x} - g_{15}\frac{\partial F}{\partial y}\right) \times -\frac{dx}{ds}] \times ds = 2 \times A_{s_1} \tag{44}$$

$$\oint_{s_1} [(g_{24}\frac{\partial \phi}{\partial x} - g_{25}\frac{\partial \phi}{\partial y} - \eta_{22}\frac{\partial F}{\partial x} + \eta_{12}\frac{\partial F}{\partial y}) \times \frac{dy}{ds} + \left(-g_{14}\frac{\partial \phi}{\partial x} + g_{15}\frac{\partial \phi}{\partial y} + \eta_{12}\frac{\partial F}{\partial x} - \eta_{11}\frac{\partial F}{\partial y}\right) \times -\frac{dx}{ds}] \times ds = 0 \tag{45}$$

If cross-section has more than one hole, Eqs.(44) and (45) must satisfied for each hole

$$\oint_{s_k} [(-s_{44}\frac{\partial \phi}{\partial x} + s_{45}\frac{\partial \phi}{\partial y} - g_{24}\frac{\partial F}{\partial x} + g_{14}\frac{\partial F}{\partial y}) \times \frac{dy}{ds} + \left(+s_{45}\frac{\partial \phi}{\partial x} - s_{55}\frac{\partial \phi}{\partial y} + g_{25}\frac{\partial F}{\partial x} - g_{15}\frac{\partial F}{\partial y}\right) \times -\frac{dx}{ds}] \times ds = 2 \times A_{s_k} \tag{46}$$

$$\oint_{s_k} [(g_{24}\frac{\partial \phi}{\partial x} - g_{25}\frac{\partial \phi}{\partial y} - \eta_{22}\frac{\partial F}{\partial x} + \eta_{12}\frac{\partial F}{\partial y}) \times \frac{dy}{ds} + \left(-g_{14}\frac{\partial \phi}{\partial x} + g_{15}\frac{\partial \phi}{\partial y} + \eta_{12}\frac{\partial F}{\partial x} - \eta_{11}\frac{\partial F}{\partial y}\right) \times -\frac{dx}{ds}] \times ds = 0 \tag{47}$$

From Eqs.(41) and (42) with differentiating $(41)_1$ with respect x and $(41)_2$ with respect y and combination the results, also with differentiating $(42)_1$ with respect x and $(42)_2$ with respect y and combination the results, we have compatibility relations

$$\frac{\partial}{\partial x}\left(s_{44}\frac{\partial\phi}{\partial x}-s_{45}\frac{\partial\phi}{\partial y}+g_{24}\frac{\partial F}{\partial x}-g_{14}\frac{\partial F}{\partial y}\right)+\frac{\partial}{\partial y}\left(-s_{45}\frac{\partial\phi}{\partial x}+s_{55}\frac{\partial\phi}{\partial y}-g_{25}\frac{\partial F}{\partial x}+g_{15}\frac{\partial F}{\partial y}\right)=-2 \quad \text{in } R \tag{48}$$

$$\frac{\partial}{\partial x}\left(g_{24}\frac{\partial\phi}{\partial x}-g_{25}\frac{\partial\phi}{\partial y}-\eta_{22}\frac{\partial F}{\partial x}+\eta_{12}\frac{\partial F}{\partial y}\right)+\frac{\partial}{\partial y}\left(-g_{14}\frac{\partial\phi}{\partial x}+g_{15}\frac{\partial\phi}{\partial y}+\eta_{12}\frac{\partial F}{\partial x}-\eta_{11}\frac{\partial F}{\partial y}\right)=0 \quad \text{in } R \tag{49}$$

2.2.2 Torsional rigidity

The torsional rigidity of the piezoelectric beam is obtained from below equation [7]

$$T=\iint_R x\,\tau_{yz}-y\,\tau_{xz}=-\alpha\iint_R\left(x\frac{\partial\phi}{\partial x}+y\frac{\partial\phi}{\partial y}\right)dxdy \tag{50}$$

By the using green's theorem and boundary conditions for multiply connected cross-sections, it can be written

$$\iint_R x\frac{\partial\phi}{\partial x}dxdy=\iint_R\frac{\partial}{\partial x}(x\,\phi)dxdy-\iint_R\phi dxdy=\oint_s x\,\phi n_x ds-\iint_R\phi dxdy \tag{51}$$

$$\iint_R y\frac{\partial\phi}{\partial y}dxdy=\iint_R\frac{\partial}{\partial y}(y\,\phi)dxdy-\iint_R\phi dxdy=\oint_s y\,\phi n_y ds-\iint_R\phi dxdy \tag{52}$$

$$T=2\alpha(\iint_R\phi dxdy+\sum_{k=1}^{N}\phi_i A_i \tag{53}$$

and torsional rigidity defined as [41,7]

$$J=\frac{T}{\alpha}=2(\iint_R\phi dxdy+\sum_{k=1}^{N}\phi_i A_i) \tag{54}$$

with multiplying Eq.(48) with ϕ and Eq.(49) with F and using the green's theorem and summing the results by getting integral have

$$\begin{aligned}&2(\iint_R\phi dxdy+\sum_{k=1}^{N}\phi_i A_i)-\iint_R[(s_{44}\frac{\partial\phi}{\partial x}\frac{\partial\phi}{\partial x}-s_{45}\frac{\partial\phi}{\partial x}\frac{\partial\phi}{\partial y}-s_{45}\frac{\partial\phi}{\partial y}\frac{\partial\phi}{\partial x}+s_{55}\frac{\partial\phi}{\partial y}\frac{\partial\phi}{\partial y})\\&+2\left(g_{24}\frac{\partial\phi}{\partial x}\frac{\partial F}{\partial x}-g_{14}\frac{\partial\phi}{\partial x}\frac{\partial F}{\partial y}-g_{25}\frac{\partial\phi}{\partial y}\frac{\partial F}{\partial x}+g_{15}\frac{\partial\phi}{\partial y}\frac{\partial F}{\partial y}\right)\\&-\left(\eta_{22}\frac{\partial F}{\partial x}\frac{\partial F}{\partial x}-\eta_{12}\frac{\partial F}{\partial x}\frac{\partial F}{\partial y}-\eta_{12}\frac{\partial F}{\partial y}\frac{\partial F}{\partial x}+\eta_{11}\frac{\partial F}{\partial y}\frac{\partial F}{\partial y}\right)]dxdy=0\end{aligned} \tag{55}$$

By the combination the Eq.(54) with Eq.(55),we have new formula for the torsional rigidity for simply connected

$$J=\iint_R[(s_{44}\frac{\partial\phi}{\partial x}\frac{\partial\phi}{\partial x}-s_{45}\frac{\partial\phi}{\partial x}\frac{\partial\phi}{\partial y}-s_{45}\frac{\partial\phi}{\partial y}\frac{\partial\phi}{\partial x}+s_{55}\frac{\partial\phi}{\partial y}\frac{\partial\phi}{\partial y}) +2\left(g_{24}\frac{\partial\phi}{\partial x}\frac{\partial F}{\partial x}-g_{14}\frac{\partial\phi}{\partial x}\frac{\partial F}{\partial y}-g_{25}\frac{\partial\phi}{\partial y}\frac{\partial F}{\partial x}+g_{15}\frac{\partial\phi}{\partial y}\frac{\partial F}{\partial y}\right) -\left(\eta_{22}\frac{\partial F}{\partial x}\frac{\partial F}{\partial x}-\eta_{12}\frac{\partial F}{\partial x}\frac{\partial F}{\partial y}-\eta_{12}\frac{\partial F}{\partial y}\frac{\partial F}{\partial x}+\eta_{11}\frac{\partial F}{\partial y}\frac{\partial F}{\partial y}\right)]dxdy \tag{56}$$

The torque of electric displacement field is defined as [33,34,7]

$$T_D=\iint_R xD_y-yD_x=-\alpha\iint_R(x\frac{\partial F}{\partial x}+y\frac{\partial F}{\partial y})dxdy \tag{57}$$

$$\iint_R x\frac{\partial F}{\partial x}dxdy=\iint_R\frac{\partial}{\partial x}(xF)dxdy-\iint_R Fdxdy=\oint_s xFn_x ds-\iint_R Fdxdy \tag{58}$$

$$\iint_R y\frac{\partial F}{\partial y}dxdy=\iint_R\frac{\partial}{\partial y}(yF)dxdy-\iint_R Fdxdy=\oint_s yFn_y ds-\iint_R Fdxdy \tag{59}$$

$$T_D=2\alpha(\iint_R Fdxdy+\sum_{k=1}^{N}F_iA_i) \tag{60}$$

The electrical torsional rigidity J_D defined as [33,34,7]

$$J_D=\frac{T_D}{\alpha}=2(\iint_R Fdxdy+\sum_{k=1}^{N}F_iA_i) \tag{61}$$

with multiplying Eq.(48) with F and Eq.(49) with ϕ and using the green's theorem and getting integral we have

$$2(\iint_R Fdxdy+\sum_{k=1}^{N}F_iA_i)-\iint_R[(s_{44}\frac{\partial F}{\partial x}\frac{\partial\phi}{\partial x}-s_{45}\frac{\partial F}{\partial x}\frac{\partial\phi}{\partial y}-s_{45}\frac{\partial F}{\partial y}\frac{\partial\phi}{\partial x}+s_{55}\frac{\partial F}{\partial y}\frac{\partial\phi}{\partial y}) +\left(g_{24}\frac{\partial F}{\partial x}\frac{\partial F}{\partial x}-g_{14}\frac{\partial F}{\partial x}\frac{\partial F}{\partial y}-g_{25}\frac{\partial F}{\partial y}\frac{\partial F}{\partial x}+g_{15}\frac{\partial F}{\partial y}\frac{\partial F}{\partial y}\right)]dxdy=0 \tag{62}$$

By the combination the Eq.(61) with Eq.(62),we have new formula for the electrical torsional rigidity for simply connected

$$J_D=\iint_R[(s_{44}\frac{\partial F}{\partial x}\frac{\partial\phi}{\partial x}-s_{45}\frac{\partial F}{\partial x}\frac{\partial\phi}{\partial y}-s_{45}\frac{\partial F}{\partial y}\frac{\partial\phi}{\partial x}+s_{55}\frac{\partial F}{\partial y}\frac{\partial\phi}{\partial y}) +\left(g_{24}\frac{\partial F}{\partial x}\frac{\partial F}{\partial x}-g_{14}\frac{\partial F}{\partial x}\frac{\partial F}{\partial y}-g_{25}\frac{\partial F}{\partial y}\frac{\partial F}{\partial x}+g_{15}\frac{\partial F}{\partial y}\frac{\partial F}{\partial y}\right)]dxdy \tag{63}$$

Electrical boundary conditions if piezo layer be actuator is as follow [2]

$$\psi=V \quad \text{at} \quad r=r_0 \tag{64}$$

If piezo layer be sensor is as follow:

$$\psi = \text{Influence of actuator layer at } r = r_0 \tag{65}$$

In addition, the electric potential, ψ , at inner surface of the piezo is also zero [2].

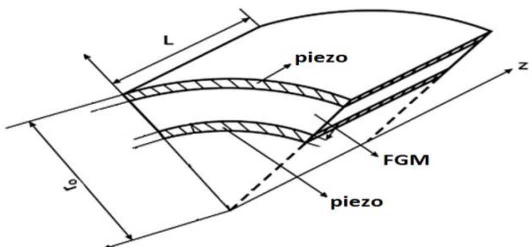

Fig.2
Geometry of Piezo-FGM.

3 CONTINUITY CONDITIONS

If we have 3 layers on together Eqs.(12) and $(30)_1$ are much different(middle layer be FGM). conditions must ensure that (a) the shear stresses normal to the interface are the same in each region; and (b) the axial displacements are compatible on the interface. Here also a additional condition is examined. The first of these can be expressed as [1,42]

$$\left[\tau_{xz} n_x + \tau_{yz} n_y\right]_{Inner\ Piezo} = \left[\tau_{xz} n_x + \tau_{yz} n_y\right]_{FGM} \tag{66}$$

$$\left[\tau_{xz} n_x + \tau_{yz} n_y\right]_{FGM} = \left[\tau_{xz} n_x + \tau_{yz} n_y\right]_{Outer\ Piezo} \tag{67}$$

$$\left(\frac{d\phi}{ds}\right)_{Inner\ Piezo} = \left(\frac{1}{\alpha}\frac{d\phi}{ds}\right)_{FGM} \tag{68}$$

$$\left(\frac{1}{\alpha}\frac{d\phi}{ds}\right)_{FGM} = \left(\frac{d\phi}{ds}\right)_{Outer\ Piezo} \tag{69}$$

On the external and internal boundaries we have

$$\tau_{xz} n_x + \tau_{yz} n_y = 0 \tag{70}$$

$$\frac{\partial\phi}{\partial x}\frac{dx}{ds} + \frac{\partial\phi}{\partial y}\frac{dy}{ds} = 0 \tag{71}$$

$$\frac{d\phi}{ds} = 0 \tag{72}$$

$$\phi = 0 \tag{73}$$

The second condition is satisfied [42]

$$\left(\frac{\partial\omega}{\partial s}\right)_{Inner\ Piezo} = \left(\frac{1}{\alpha}\frac{\partial\omega}{\partial s}\right)_{FGM} \tag{74}$$

$$(\frac{1}{\alpha}\frac{\partial\omega}{\partial s})_{FGM}=(\frac{\partial\omega}{\partial s})_{Outer\ Piezo} \tag{75}$$

$$\left(+s_{55}\frac{\partial\phi}{\partial y}\frac{dy}{dn}-s_{45}\frac{d\phi}{ds}+s_{44}\frac{\partial\phi}{\partial x}\frac{dx}{dn}+g_{15}\frac{\partial F}{\partial y}\frac{dy}{dn}+g_{25}\frac{\partial F}{\partial x}\frac{dx}{ds}-g_{14}\frac{\partial F}{\partial y}\frac{dy}{ds}+g_{24}\frac{\partial F}{\partial x}\frac{dx}{dn}\right)_{Inner\ piezo}=\left(\frac{1}{\alpha}\frac{1}{\mu}\frac{d\phi}{dn}\right)_{FGM} \tag{76}$$

$$\left(\frac{1}{\alpha}\frac{1}{\mu}\frac{d\phi}{dn}\right)_{FGM}=\left(+s_{55}\frac{\partial\phi}{\partial y}\frac{dy}{dn}-s_{45}\frac{d\phi}{ds}+s_{44}\frac{\partial\phi}{\partial x}\frac{dx}{dn}+g_{15}\frac{\partial F}{\partial y}\frac{dy}{dn}+g_{25}\frac{\partial F}{\partial x}\frac{dx}{ds}-g_{14}\frac{\partial F}{\partial y}\frac{dy}{ds}+g_{24}\frac{\partial F}{\partial x}\frac{dx}{dn}\right)_{Outer\ piezo} \tag{77}$$

If the material piezoelectric be Transversely Isotropic have

$$g_{14}=g_{25}=s_{45}=\eta_{12}=0,\quad s_{44}=s_{55},\ g_{24}=g_{15}\ ,\ \eta_{11}=\eta_{22} \tag{78}$$

$$\left(s_{55}\frac{d\phi}{dn}+g_{15}\frac{dF}{dn}\right)_{Inner\ piezo}=\left(\frac{1}{\alpha}\frac{1}{\mu}\frac{d\phi}{dn}\right)_{FGM} \tag{79}$$

$$\left(\frac{1}{\alpha}\frac{1}{\mu}\frac{d\phi}{dn}\right)_{FGM}=\left(s_{55}\frac{d\phi}{dn}+g_{15}\frac{dF}{dn}\right)_{Outer\ piezo} \tag{80}$$

and now an additional condition would be required (in this state assumed material piezoelectric be Transversely Isotropic)[42]

$$\oint_{R_1}\left(s_{55}\frac{d\phi}{dn}+g_{15}\frac{dF}{dn}\right)_{Inner\ piezo}=\oint_{R_2}\left(\frac{1}{\alpha}\frac{1}{\mu}\frac{d\phi}{dn}\right)_{FGM} \tag{81}$$

$$\oint_{R_2}\left(\frac{1}{\alpha}\frac{1}{\mu}\frac{d\phi}{dn}\right)_{FGM}=\oint_{R_3}\left(s_{55}\frac{d\phi}{dn}+g_{15}\frac{dF}{dn}\right)_{Outer\ piezo} \tag{82}$$

$$\iint_{R_1}[s_{55}(\frac{\partial^2\phi}{\partial x^2}+\frac{\partial^2\phi}{\partial y^2})+g_{15}\left(\frac{\partial^2 F}{\partial x^2}+\frac{\partial^2 F}{\partial y^2}\right)]dxdy=\oint_{R_2}\left(\frac{1}{\alpha}\frac{1}{\mu}\frac{d\phi}{dn}\right)_{FGM} \tag{83}$$

$$\oint_{R_2}\left(\frac{1}{\alpha}\frac{1}{\mu}\frac{d\phi}{dn}\right)_{FGM}=\iint_{R_3}[s_{55}(\frac{\partial^2\phi}{\partial x^2}+\frac{\partial^2\phi}{\partial y^2})+g_{15}\left(\frac{\partial^2 F}{\partial x^2}+\frac{\partial^2 F}{\partial y^2}\right)]dxdy \tag{84}$$

$$\left(-2A_1\right)_{Inner\ piezo}=\oint_{R_2}\left(\frac{1}{\alpha}\frac{1}{\mu}\frac{d\phi}{dn}\right)_{FGM} \tag{85}$$

$$\oint_{R_2}\left(\frac{1}{\alpha}\frac{1}{\mu}\frac{d\phi}{dn}\right)_{FGM}=\left(-2A_3\right)_{Outer\ piezo} \tag{86}$$

4 EXAMPLE

Fig.3 shows the considered FGM hollow circular cross-section which is bounded by 2 concentric hollow piezo layers.

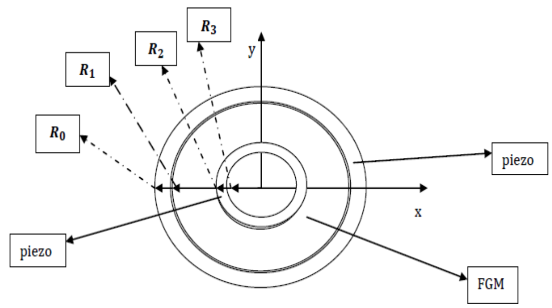

Fig.3
Hollow circular cross-section piezo-FGM under the Torsion.

$$\phi_{1(\boldsymbol{outer\ piezo\ layer})} = \boldsymbol{k}_1\left(\boldsymbol{R}_0^{\ 2} - \boldsymbol{x}^2 - \boldsymbol{y}^2\right) \qquad \boldsymbol{F}_{1(\boldsymbol{outer\ piezo\ layer})} = k_2\left(R_0^{\ 2} - x^2 - y^2\right) \tag{87}$$

By substitution Prandtl's stress function and electric displacement potential function into Eq.(48) and Eq.(49) have

$$k_1 = \frac{1}{\hat{s} + \dfrac{\hat{g}^2}{\hat{\eta}}} \ , k_2 = \frac{1}{\hat{g} + \dfrac{\hat{s}\hat{\eta}}{\hat{g}}} \ , \hat{s} = s_{44} + s_{55} \ , \hat{g} = g_{24} + g_{15} \ , \hat{\eta} = \eta_{11} + \eta_{22} \tag{88}$$

$$\phi_{1(\boldsymbol{outer\ piezo\ layer})} = \frac{R_0^{\ 2} - x^2 - y^2}{\hat{s} + \dfrac{\hat{g}^2}{\hat{\eta}}} \ , \boldsymbol{F}_{1(\boldsymbol{outer\ piezo\ layer})} = \frac{R_0^{\ 2} - x^2 - y^2}{\hat{g} + \dfrac{\hat{s}\hat{\eta}}{\hat{g}}} \tag{89}$$

$$\tau_{xz} = \alpha\frac{\partial\phi_1}{\partial y} = \frac{-2\alpha y}{\hat{s} + \dfrac{\hat{g}^2}{\hat{\eta}}} \ , \tau_{yz} = -\alpha\frac{\partial\phi_1}{\partial x} = \frac{2\alpha x}{\hat{s} + \dfrac{\hat{g}^2}{\hat{\eta}}} \ , D_x = \alpha\frac{\partial F_1}{\partial y} = \frac{-2\alpha y}{\hat{g} + \dfrac{\hat{s}\hat{\eta}}{\hat{g}}} \ , D_y = -\alpha\frac{\partial F_1}{\partial x} = \frac{2\alpha x}{\hat{g} + \dfrac{\hat{s}\hat{\eta}}{\hat{g}}} \tag{90}$$

$$E_x = -g_{15}\frac{-2\alpha y}{\hat{s} + \dfrac{\hat{g}^2}{\hat{\eta}}} + \eta_{11}\frac{-2\alpha y}{\hat{g} + \dfrac{\hat{s}\hat{\eta}}{\hat{g}}} , E_y = -g_{24}\frac{2\alpha x}{\hat{s} + \dfrac{\hat{g}^2}{\hat{\eta}}} + \eta_{22}\frac{2\alpha x}{\hat{g} + \dfrac{\hat{s}\hat{\eta}}{\hat{g}}} \tag{91}$$

$$\tau = \sqrt{\tau_{xz}^{\ 2} + \tau_{yz}^{\ 2}} \ , D = \sqrt{D_x^{\ 2} + D_y^{\ 2}} \ , E = \sqrt{E_x^{\ 2} + E_y^{\ 2}} \tag{92}$$

$$J = \frac{R_0^{\ 4} - R_1^{\ 4}}{\hat{s} + \dfrac{\hat{g}^2}{\hat{\eta}}}\pi \ , J_D = \frac{R_0^{\ 4} - R_1^{\ 4}}{\hat{g} + \dfrac{\hat{s}\hat{\eta}}{\hat{g}}}\pi \tag{93}$$

$$\phi_{2(\boldsymbol{FGM\ layer})} = \frac{\boldsymbol{k}_3}{\boldsymbol{k}_4}\left(\boldsymbol{exp}\left(\boldsymbol{k}_4\left(\boldsymbol{R}_2^{\ 2} - \boldsymbol{x}^2 - \boldsymbol{y}^2\right)\right) - 1\right)\boldsymbol{\alpha} + \frac{\boldsymbol{k}_5}{\boldsymbol{k}_6}\left(\boldsymbol{exp}\left(\boldsymbol{k}_6\left(\boldsymbol{R}_1^{\ 2} - \boldsymbol{x}^2 - \boldsymbol{y}^2\right)\right) - 1\right)\boldsymbol{\alpha} \tag{94}$$

$$\begin{aligned} &\frac{\partial}{\partial x}\left(\frac{1}{\mu}\left(k_3 exp\left(k_4\left(R_2^{\ 2} - x^2 - y^2\right)\right).(-2x) + k_5 exp\left(k_6\left(R_1^{\ 2} - x^2 - y^2\right)\right).(-2x)\right)\right)\alpha \\ &+ \frac{\partial}{\partial y}\left(\frac{1}{\mu}\left(k_3 exp\left(k_4\left(R_2^{\ 2} - x^2 - y^2\right)\right).(-2y)\right) + \left(k_5 exp\left(k_6\left(R_1^{\ 2} - x^2 - y^2\right)\right).(-2y)\right)\right)\alpha = -2\alpha \end{aligned} \tag{95}$$

$$\mu = 2k_3 exp\left(k_4\left(R_2^{\,2}-x^2-y^2\right)\right)+2k_5 exp\left(k_6\left(R_1^{\,2}-x^2-y^2\right)\right) \tag{96}$$

$$\tau_{xz} = \frac{\partial \phi_2}{\partial y} = -2k_3 exp\left(k_4\left(R_2^{\,2}-x^2-y^2\right)\right)\alpha y - 2k_5 exp\left(k_6\left(R_1^{\,2}-x^2-y^2\right)\right)\alpha y \tag{97}$$

$$\tau_{yz} = -\frac{\partial \phi_2}{\partial x} = 2k_3 exp\left(k_4\left(R_2^{\,2}-x^2-y^2\right)\right)\alpha x + 2k_5 exp\left(k_6\left(R_1^{\,2}-x^2-y^2\right)\right)\alpha x \tag{98}$$

$$\tau = \sqrt{\tau_{xz}^{\,2}+\tau_{yz}^{\,2}} \tag{99}$$

Eqs.(46) and (47),(24) are satisfied.

$$J = 2\left(\iint_R \phi_2 dxdy + \phi_2 A_2 + \phi_2 A_1\right)$$

$$J = -2\pi\left(\frac{R_1^{\,2}k_3}{k_4}-\frac{R_2^{\,2}k_3}{k_4}+\frac{R_1^{\,2}k_5}{k_6}-\frac{R_2^{\,2}k_5}{k_6}+\frac{k_3\left(\exp\left(R_2^{\,2}k_4-R_1^{\,2}k_4\right)-1\right)}{k_4^{\,2}}-\frac{k_5\left(\exp\left(R_1^{\,2}k_6-R_2^{\,2}k_6\right)-1\right)}{k_6^{\,2}}\right) \tag{100}$$

$$-2\left(\frac{k_3}{k_4}\right)\left(\exp\left(k_4R_2^{\,2}-k_4R_1^{\,2}\right)-1\right)\pi\left(R_1^{\,2}\right)+2\left(\frac{k_5}{k_6}\right)\left(\exp\left(k_6R_1^{\,2}-k_6R_2^{\,2}\right)-1\right)\pi\left(R_2^{\,2}\right)$$

$$\phi_{3(\textbf{\textit{inner piezo layer}})} = \boldsymbol{k}_7\left(\boldsymbol{R}_3^{\,2}-\boldsymbol{x}^2-\boldsymbol{y}^2\right) \qquad \boldsymbol{F}_{3(\textbf{\textit{inner piezo layer}})} = k_8\left(R_3^{\,2}-x^2-y^2\right) \tag{101}$$

$$k_7 = \frac{1}{\hat{s}+\frac{\hat{g}^2}{\hat{\eta}}} \quad ,k_8 = \frac{1}{\hat{g}+\frac{\hat{s}\hat{\eta}}{\hat{g}}} ,\hat{s} = s_{44}+s_{55} ,\hat{g} = g_{24}+g_{15} ,\hat{\eta} = \eta_{11}+\eta_{22} \tag{102}$$

$$\phi_{3(\textbf{\textit{inner piezo layer}})} = \frac{R_3^{\,2}-x^2-y^2}{\hat{s}+\frac{\hat{g}^2}{\hat{\eta}}} \ , \boldsymbol{F}_{3(\textbf{\textit{inner piezo layer}})} = \frac{R_3^{\,2}-x^2-y^2}{\hat{g}+\frac{\hat{s}\hat{\eta}}{\hat{g}}} \tag{103}$$

$$\tau_{xz} = \alpha\frac{\partial \phi_3}{\partial y} = \frac{-2\alpha y}{\hat{s}+\frac{\hat{g}^2}{\hat{\eta}}} \ ,\tau_{yz} = -\alpha\frac{\partial \phi_3}{\partial x} = \frac{2\alpha x}{\hat{s}+\frac{\hat{g}^2}{\hat{\eta}}} \ ,D_x = \alpha\frac{\partial F_3}{\partial y} = \frac{-2\alpha y}{\hat{g}+\frac{\hat{s}\hat{\eta}}{\hat{g}}} ,D_y = -\alpha\frac{\partial F_3}{\partial x} = \frac{2\alpha x}{\hat{g}+\frac{\hat{s}\hat{\eta}}{\hat{g}}} \tag{104}$$

$$E_x = -g_{15}\frac{-2\alpha y}{\hat{s}+\frac{\hat{g}^2}{\hat{\eta}}}+\eta_{11}\frac{-2\alpha y}{\hat{g}+\frac{\hat{s}\hat{\eta}}{\hat{g}}} ,E_y = -g_{24}\frac{2\alpha x}{\hat{s}+\frac{\hat{g}^2}{\hat{\eta}}}+\eta_{22}\frac{2\alpha x}{\hat{g}+\frac{\hat{s}\hat{\eta}}{\hat{g}}} \tag{105}$$

$$\tau = \sqrt{\tau_{xz}^{\,2}+\tau_{yz}^{\,2}} \ ,D = \sqrt{D_x^{\,2}+D_y^{\,2}} \ ,E = \sqrt{E_x^{\,2}+E_y^{\,2}} \tag{106}$$

$$J = \frac{R_2^{\,4}-R_3^{\,4}}{\hat{s}+\frac{\hat{g}^2}{\hat{\eta}}}\pi \ ,J_D = \frac{R_2^{\,4}-R_3^{\,4}}{\hat{g}+\frac{\hat{s}\hat{\eta}}{\hat{g}}}\pi \tag{107}$$

In this example torsional function and electric potential are zero. Continuously Conditions

$$\left(\frac{1}{\bar{s}+\frac{\bar{g}^2}{\bar{\eta}}}\right)_{outer\ piezo\ layer} = k_3 exp\left(k_4\left(R_2{}^2-R_1{}^2\right)\right)+k_5 \tag{108}$$

$$k_5 exp\left(k_6\left(R_1{}^2-R_2{}^2\right)\right)+k_3=\left(\frac{1}{\bar{s}+\frac{\bar{g}^2}{\bar{\eta}}}\right)_{inner\ piezo\ layer} \tag{109}$$

Also relations (74),(75) and (81),(82) are satisfied.

5 RESULTS AND DISCUSSION

Consider a FGM hollow circular cross-section which is bounded by 2 concentric hollow piezo layers, where $R_0=0.68m$, $R_1=0.64m$, $R_2=0.44m$, $R_3=0.40m$. The shear modulus of FGM is a exponential function which is 25 *GPa* and 21 *Gpa* at inner and outer surfaces respectively. Properties of piezoelectric materials is base on the Table 1. Outer piezo layer and inner piezo layer are PZT-5H and PZT-4 respectively. The piezo-FGM panel is under the $3\times10^4 N.m$ Torque.

Table 1
Material properties of piezoelectric.

Property	$s_{44}(10^{-12}m^2/N)$	$s_{55}(10^{-12}m^2/N)$	$g_{15}(10^{-3}m^2/C)$	$g_{24}(10^{-3}m^2/C)$	$\eta_{11}\left(10^6 m/F\right)$	$\eta_{22}\left(10^6 m/F\right)$
PZT-5H	43.5	43.5	29	29	66.4	66.4
PZT-4	17.9	17.9	40	40	76.87	76.87

Figs. 4,5,6 and 8,9,10 shows shear stress and electric displacement for outer piezo layer respectively, Figs. 7 and 11 shows shear stress contours for Fig. 6 and electric displacement contours for Fig. 10 respectively. Figs. 12,13,14 shows shear stress for FGM layer, Fig. 15 shows shear stress contours for Fig. 14. Figs. 16,17,18 and 20,21,22 shows shears stress and electric displacement for inner piezo layer respectively, Figs. 19 and 23 shows shear stress contours for Fig. 18 and electric displacement contours for Fig. 22 respectively. Dotted lines indicate positive values of shear stress. Electric potential function and torsional function due to symmetry are zero. Fig. 24 shows electric potential and torsional function form for elliptical cross-section and Fig. 25 shows electric potential and torsional function contours for Fig. 24, solid lines correspond to negative values of *w*, indicating that points move in of the section in the negative *z* direction, while dotted lines indicate positive values of displacement, along each of the coordinate axes the torsional function is zero. Figs. 26,27,28 Shows the effect of the piezoelectric layers on the mechanical behavior of FGM depends on its thickness and with the increases the piezoelectric layers thickness decrease the stresses in the FGM layer,and if thickness of piezo be small(for example thickness of piezo be 1/100 FGM)it effect can be neglected. From the compare Figs. 4,5,6 with 8,9,10 or 16,17,18 with 20,21,22 respectively have this result that Increasing the shear stress causes to increase the electric displacement. In Figs. 12-14, if material was homogeneous instead of non-homogeneous, increase the maximum value of stress, so from the study we have, functionally graded materials causes to decrease the maximum value of stresses in comparison with the homogeneous material. base on the Membrane Analogy for homogeneous state the maximum shear stress appears always to occur on the boundary where the largest slope of the membrane occurs [2], as we came to the conclusion that where the maximum shear stress, electric displacement is the maximum, as from compare Figs. 6,7 with 10,11 or 18,19 with 22,23. This result is confirmed. As mentioned maximum shear stress occurs at the outer boundary for all homogeneous cylinders with any cross-section geometry (like Figs. 4-6 and 16-18) but in non-homogeneous, maximum shear stress can occur at the anywhere in cross-section. Influence of electrical torsional torque is very low in compare torsional torque. For circular cross-sections relations 64,65 have no apply (because electric potential function is zero).

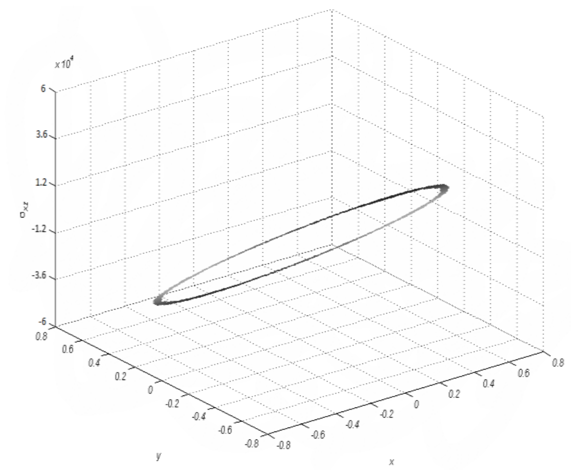

Fig.4
Shear stress for outer piezo layer.

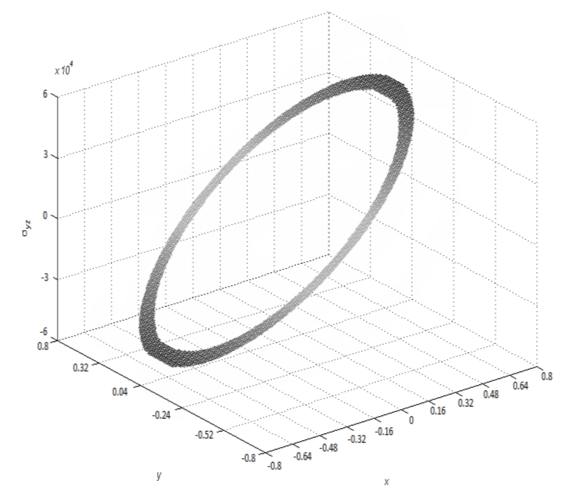

Fig.5
Shear stress for outer piezo layer.

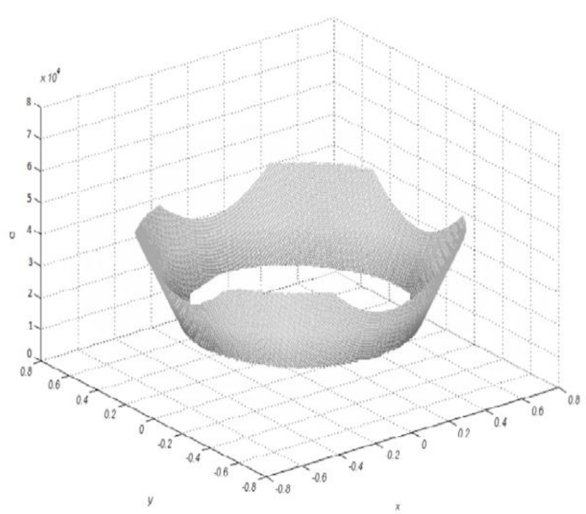

Fig.6
Shear stress for outer piezo layer.

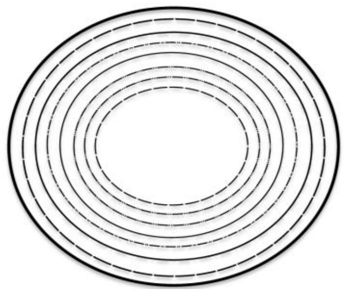

Fig.7
Shear stress contours for Fig. 6.

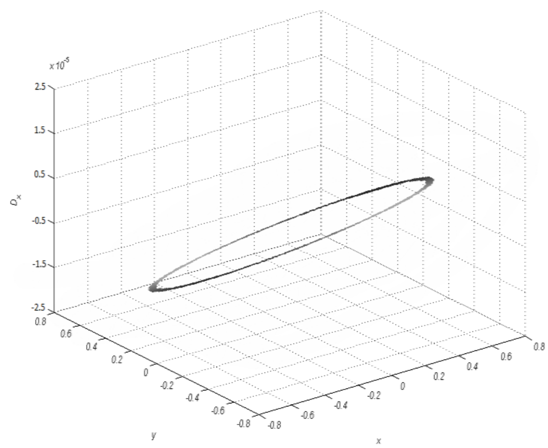

Fig.8
Electric displacement for outer piezo layer.

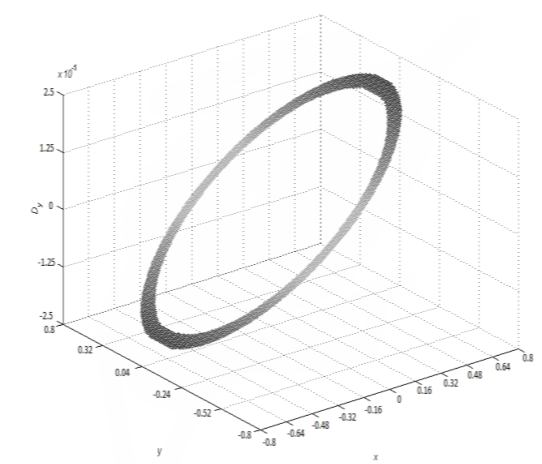

Fig.9
Electric displacement for outer piezo layer.

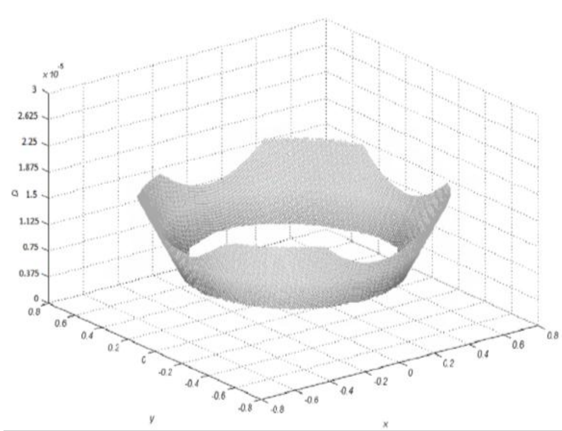

Fig.10
Electric displacement for outer piezo layer.

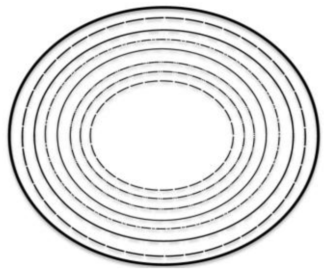

Fig.11
Electric displacement contours for Fig. 10.

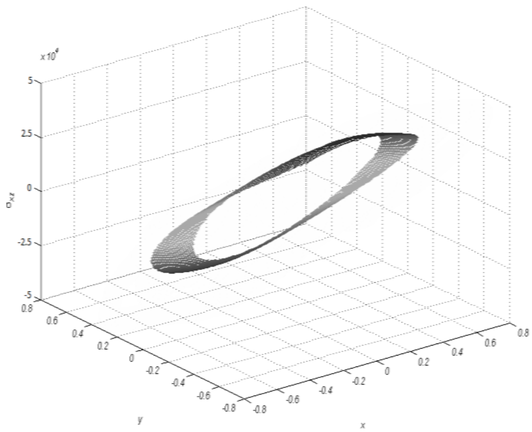

Fig.12
Shear stress for FGM layer.

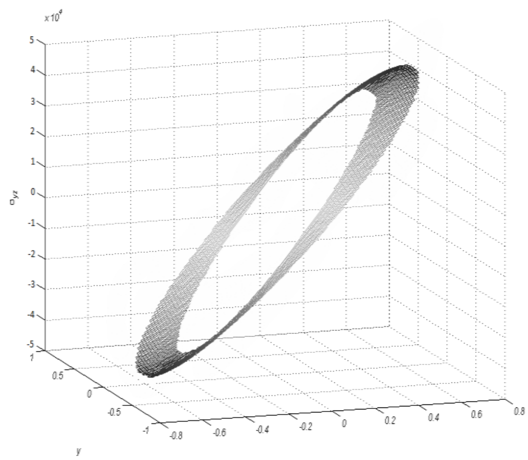

Fig.13
Shear stress for FGM layer.

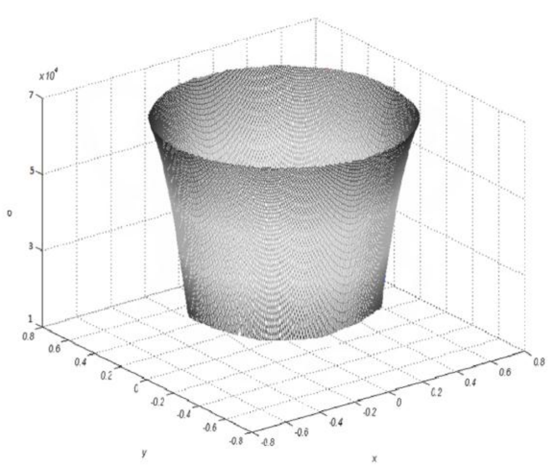

Fig.14
Shear stress for FGM layer.

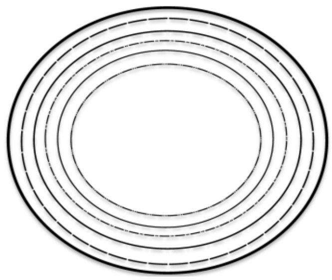

Fig.15
Shear stress contours for Fig.14.

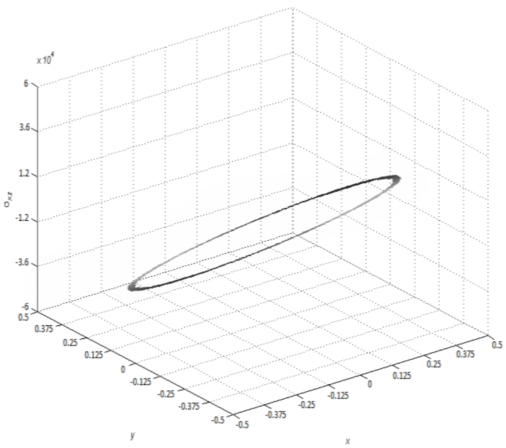

Fig.16
Shear stress for inner piezo layer.

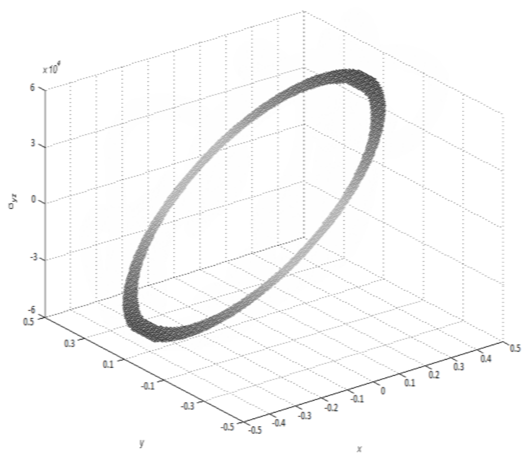

Fig.17
Shear stress for inner piezo layer.

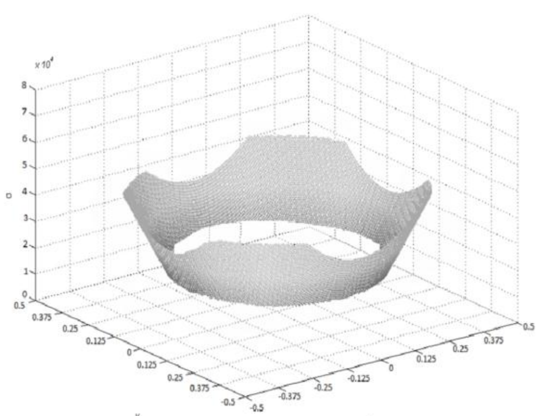

Fig.18
Shear stress for inner piezo layer.

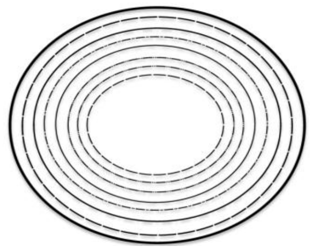

Fig.19
Shear stress contours for Fig. 18.

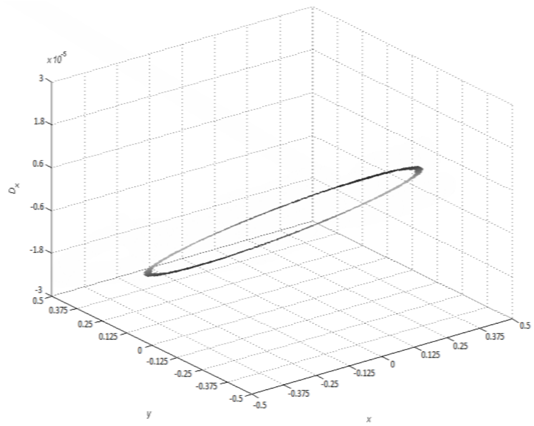

Fig.20
Electric displacement for inner piezo layer.

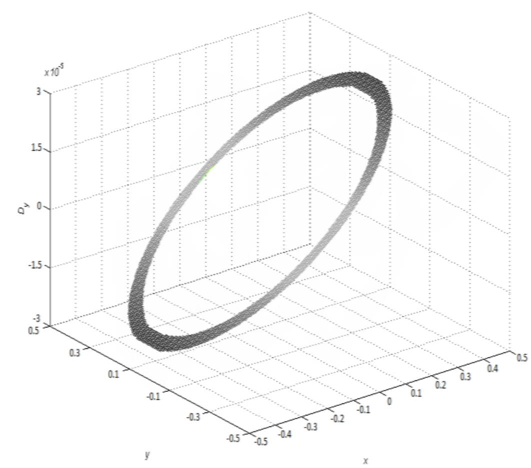

Fig.21
Electric displacement for inner piezo layer.

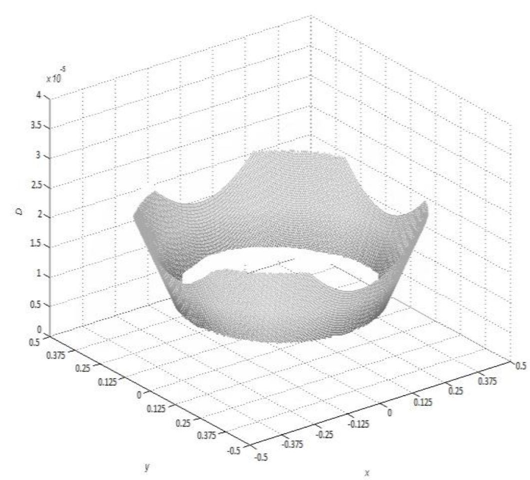

Fig.22
Electric displacement for inner piezo layer.

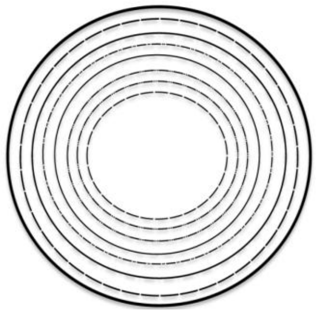

Fig.23
Electric displacement contours for Fig. 22.

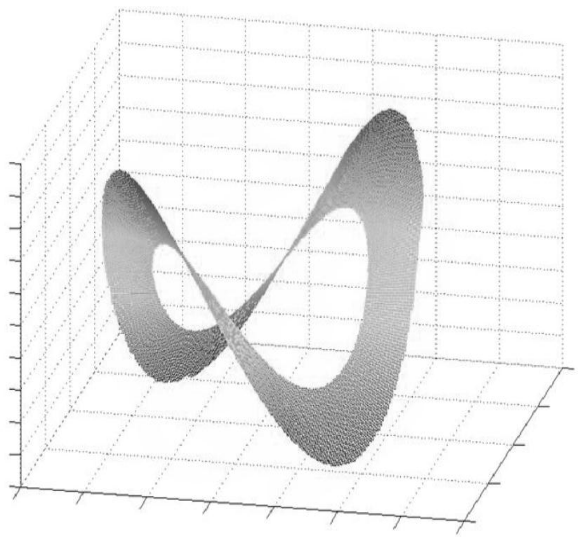

Fig.24
Electric potential and torsional function form for elliptical cross-section.

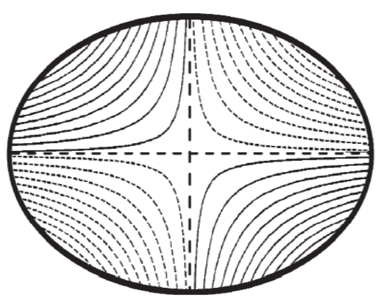

Fig.25
Electric potential and torsional function contours for Fig. 24.

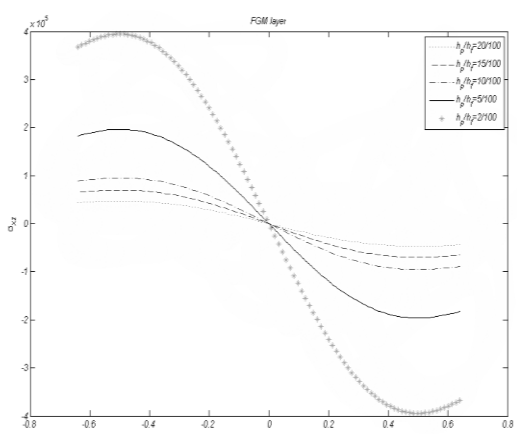

Fig.26
Influence of piezoelectric layers thickness on mechanical behavior of FGM.

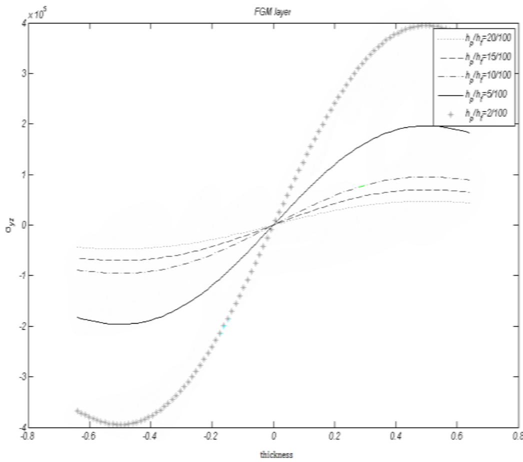

Fig.27
Influence of piezoelectric layers thickness on mechanical behavior of FGM.

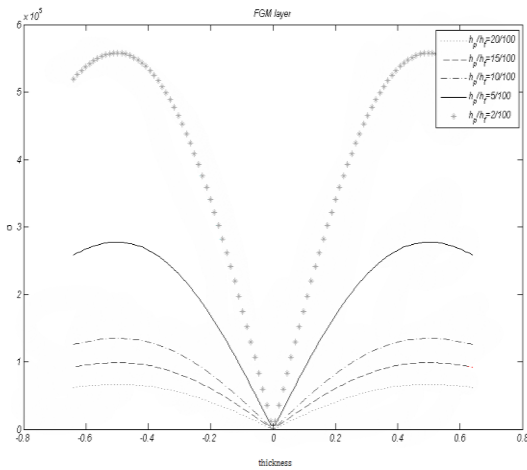

Fig.28
Influence of piezoelectric layers thickness on mechanical behavior of FGM.

6 CONCLUSION

In this paper elasticity solution for an FGM cylindrical shaft with piezoelectric layers in the framework of the linear theory elasticity and piezoelectricity under the torsion by using Prandtl's formulation is presented. The numerical results have revealed that the material inhomogeneity and piezoelectric layers have an important effect on the elastic fields in the cylindrical panel. The paper generalizes the known elastic solution of torsional problem developed by Prandtl to homogeneous piezoelectric and elastic, isotropic non-homogeneous shafts. the continuity and compatibility conditions are satisfied. This method is Exact analytical solution for solid circular cross-section but this method is approximate solution for thin-walled cross-sections.one example with solution illustrate the applications of presented formulations.

REFERENCES

[1] Rooney J.F., Ferrari M.,1995, Torsion and flexure of inhomogeneous elements, *Composites Engineering* **5**: 901-911.

[2] Alibeigloo A., Chen W.Q., 2010, Elasticity solution for an FGM cylindrical panel integrated with piezoelectric layers, *Europen Journal of Mechanics A/Solids* **29**: 714-723.

[3] Arghavan S., Hematiyan M.R., 2009, Torsion of functionally graded hollow tubes, *European Journal Mechanics A/Solids* **28**(3): 551-559.

[4] Talebanpour A., Hematiyan M.R., 2014, Torsional analysis of piezoelectric hollow bars, *International Journal of Applied Mechanics* **6**(2): 1450019.

[5] Gurel M.A., Pekgökgöz R.K., Kisa M., 2008, Approximate torsion analysis of closed moderately thick-walled, thick-walled, and solid cross-sections, *Turkish Journal of Engineering and Environmental Sciences* **32(5)**: 277-287.

[6] Tarn J.Q., Chang H.H., 2007, Torsion of cylindrically orthotropic elastic circular bars with radial inhomogeneity: some exact solutions and end effects, *International Journal of Solids and Structures* **45**: 303-319.

[7] Ecsedi I., Baksa A., 2010, Prandtl's formulation for the saint-venant's of homogeneous piezoelectric beams, *International Journal of Solids and Structures* **47**:3076-3083.

[8] Higgins T.J., 1942, A comprehensive review of Saint-Venant torsion problem, *American Journal of Physics* **10**: 248-259.

[9] Timoshenko S.P., Goodier J.N., 1970, *Theory of Elasticity*, McGraw-Hill, New York.

[10] Sokolnikoff I.S., 1956, *Mathematical Theory of Elasticity*, McGraw-Hill, New York.

[11] Chen T., 2011, A novel class of graded cylinders neutral to host shafts of arbitrary cross-sections under torsion, *Mechanics Research Communications* **38**: 68-71.

[12] Baron F.M., 1942, Torsion of multi-connected thin-walled cylinders, *Journal of Applied Mechanics* **9**: 72-74.

[13] Li Z., Ko J.M., Ni Y.Q., 2000, Torsional rigidity of reinforced concrete bars with arbitrary sectional shape, *Finite Elements in Analysis and Design* **35**: 349-361.

[14] Mejak G., 2000, Optimization of cross-section of h ollow prismatic bars in torsion, *Communications in Numerical Methods in Engineering* **16**: 687-695.

[15] Sezawa K., Kubo K., 1931, *The Buckling of a Cylindrical Shell Inder Torsion*, Aerospace Research Institute, Tokyo Imperial University.

[16] Lundquist E., 1932, Strength Tests on Thin-Walled Duralumin Cylinders in Torsion, *NACA Technical Notes* **427**: 1-24.

[17] Doostfatemeh A., Hematiyan M.R., Arghavan S., 2009, Closed-form approximate formulations for torsional analyses of hollow tube with straight and circular edges, *Journal of Mechanics* **25**: 401-409.

[18] Muskhelishvilli N.I., 1953, *Some Basic Problems of the Mathematical Theory of Elasticity*, Groningen Holland.

[19] Booker J.R., Kitipornchai S., 1971, Torsion of multilayered rectangular section, *Journal of the Engineering Mechanics Division* **97**(EM5): 1451-1468.

[20] Kuo Y.M., Conway H.D., 1973, The torsion of composite tubes and cylinders, *International Journal of Solids and Structures* **9**(12): 1553-1565.

[21] Kuo Y.M., Conway H.D., 1974, Torsion of cylinders with multiple reinforcement, *Journal of the Engineering Mechanics Division* **100**(EM2): 221-234.

[22] Kuo Y.M., Conway H.D., 1974, Torsion of composite rhombus cylinder, *Journal of Applied Mechanics* **31**(2): 302-303.

[23] Kuo Y.M., Conway H.D., 1980, Torsion of reinforced square cylinder, *Journal of the Engineering Mechanics Division* **106**(EM6): 1341-1347.

[24] Packham B.A., Shail R., 1978, Saint- Venant torsion of composite cylinders, *Journal of Elasticity* **8**(4): 393-407.

[25] Ripton R., 1998, Optimal fiber configurations for maximum torsional rigidity, *Archive for Rational Mechanics and Analysis* **144**(1):79-106.

[26] Herrmann L.R., 1965, Elastic torsional analysis of irregular shapes, *Journal of the Engineering Mechanics Division* **91**(EM6): 11-19.

[27] Tarn J.Q., Chang H.H., 2008, Torsion of cylindrically orthotropic elastic circular bars with radial inhomogeneity: some exact solutions and end effects, *International Journal of Solids and Structures* **45**: 303-319.

[28] Lekhnitskii S.G., 1971, *Torsion of Anisotropic and Non-Homogeneous Beams*, Fizmatlit, Moscow.

[29] Lekhnitskii S.G., 1981, *Theory of Elasticity of an Anisotropic Body*, Mir, Moscow.

[30] Bisegna P., 1998, The Saint–Venant problem in the linear theory of piezoelectricity, *Atti dei Convegni Lincei, Accademia dei Lincei* **140**: 151-165.

[31] Bisegna P., 1999, The Saint–Venant problem for monoclinic piezoelectric cylinders, *ZAMM* **78**(3): 147-165.

[32] Horgan C.O., 2007, On the torsion of functionally graded anisotropic linearly elastic bars, *IMA Journal of Applied Mathematics* **72**(5): 556-562.

[33] Rovenski V., Harash E., Abramovich H., 2006, Saint-Venant's problem for homogeneous piezoelectric beams, *Technical Notes* **967**: 1-100.

[34] Rovenski V., Harash E., Abramovich H., 2007, Saint-Venant's problem for homogeneous piezoelectric beams, *Journal of Applied Mechanics* **47**(6): 1095-1103.

[35] Yang Y.S., 2005, *Introduction to the Theory of Piezoelectricity*, Springer Verlag, New York.

[36] Tawaka T., Fudaka T., Takada T., 1987, Flexural-torsion coupling vibration control of fiber composite cantilever beam by using piezoelectric actuators, *Smart Materials and Structures* **6**: 477-484.

[37] Zehetner C., 2009, Compensation of torsional vibrations in rods by piezoelectric actuation, *Acta Mechanica* **207**(1-2): 121-133.

[38] Maleki M., Naei M.H., Hoseinian E., Babahaji A., 2010, Exact three dimensional analysis for static torsion of piezoelectric rods, *International Journal of Solids and Structures* **28**: 217-226.

[39] Sadd Martin H., 2009, *Elasticity,Theory,Applications,and Numerics* , Elsevier, USA.

[40] Prandtl L., 1903, Zur torsion von prismatischen Stäben, *Physics* **4**: 758-770.

[41] Lurje A., 1970, *Theory of Elasticity*, Fizmatlit, Moscow.

[42] Ely J.F., Zienkiewicz O.C., 1960, Torsion of compound bars a relaxation solution, *International Journal of Mechanical Sciences* **1**: 356-365.

[43] Ecsedi I., 2009, Some analytical solutions for saint-venant torsion of non-homogeneous cylindrical bars, *Europen Journal of Mechanics A/Solids* **28**: 985-990.
[44] Yang J., 2005, *An Introduction to the Theory of Piezoelectric*, Springer, USA.
[45] Horgan C.O., Chan A.M., 1999, Torsion of functionally graded isotropic linearly elastic bars, *Journal of Elasticity* **52**(2): 181-189.